Original article

DOI: 10.2478/aiht-2022-73-3658

Antioxidative, cytotoxic, and antibacterial properties of self-assembled glycine-histidine-based dipeptides with or without silver nanoparticles in bio-inspired film

Merve Eylul Kiymaci[1], Hakan Erdoğan[2], and Merve Bacanlı[3]

[1] University of Health Sciences Turkey, Gülhane Faculty of Pharmacy, Department of Pharmaceutical Microbiology, Ankara, Turkey
[2] University of Health Sciences Turkey, Gülhane Faculty of Pharmacy, Department of Pharmaceutical Chemistry, Ankara, Turkey
[3] University of Health Sciences Turkey, Gülhane Faculty of Pharmacy, Department of Pharmaceutical Toxicology, Ankara, Turkey

[Received in April 2022; Similarity Check in April 2022; Accepted in June 2022]

Recent years have seen much attention being given to self-assembly of dipeptide-based structures, especially to self-regulation of dipeptide structures with different amino acid sequences. In this study we investigated the effects of varying solvent environments on the self-assembly of glycine-histidine (Gly-His) dipeptide structures. First we determined the morphological properties of Gly-His films formed in different solvent environments with scanning electron microscopy and then structural properties with Fourier-transform infrared (FTIR) spectroscopy. In addition, we studied the effects of Gly-His films on silver nanoparticle (AgNP) formation and the antioxidant and cytotoxic properties of AgNPs obtained in this way. We also, assessed antibacterial activities of Gly-His films against Gram-negative *Escherichia coli* and *Pseudomonas aeruginosa* and Gram-positive *Staphylococcus aureus*. Silver nanoparticle-decorated Gly-His films were not significantly cytotoxic at concentrations below 2 mg/mL but had antibacterial activity. We therefore believe that AgNP-decorated Gly-His films at concentrations below 2 mg/mL can be used safely against bacteria.

KEY WORDS: Ag; antibacterial surface; *Escherichia coli*; *Pseudomonas aeruginosa*; *Staphylococcus aureus*; toxicity

Many biomolecules and other components form supramolecular structures in biological systems, most notably amino acids, peptides, and proteins in human metabolism (1–3). Particularly unique are peptide-based structures with amino acid groups connected by peptide bonds (4). However, the self-assembly processes of high molecular mass peptides and more complex protein structures is still not entirely clear (5, 6), as there are too many functional groups that interact in self-assembly. At this point, however, much can be learned from dipeptides as the simplest peptide structures (7). For example, many studies have reported diphenylalanine (Phe) dipeptide, the core recognition motif of amyloid plaques found in Alzheimer's disease and type II diabetes (8). Furthermore, many dipeptides can form different structures through their interactions and be used in various applications as bio-inspired materials (6, 9). It is therefore important to study their activities and toxic effects and try to elucidate the self-assembly processes, including the solvent effects, co-arrangement, nanoparticle effects, and different architectural and morphological properties (10) to reveal the driving forces and interactions behind spontaneous arrangement of dipeptide structures. It is also important to study their beneficial effects, as a number of biopeptides, such as glutathione (γ-Glu-Cys-Gly), carnosine (β-alanyl-L-histidine), homocarnosine (γ-aminobutyryl-L-histidine), and anserine (β-alanyl-*N*-methyl-L-histidine) are natural antioxidants (11–13).

Thanks to their self-assembly, dipeptide structures are currently used in drug release, bio-sensing studies, architecture studies with surface-enhanced Raman spectroscopy (SERS), and catalysis studies, often in combination with metallic nanoparticles, gold and silver in particular, because of their antibacterial activity (14–18). So far, polymer, lipid-based, and metallic nanoparticles (NPs) have shown antibacterial, antifungal, and antiviral activities against different microorganisms (19), and silver nanoparticles (AgNPs) are the most studied for antibacterial activity (20).

Considering that glycine-histidine (Gly-His) based dipeptides can have remarkable structures and that Gly-His films formed in the solvent environment can have different useful applications, the aim of this study was to investigate how different solvents affect dipeptide self-assembly and how the obtained structures combine with AgNPs. To this end, we studied the self-assembly of Gly-His films in $AgNO_3$ solution and the antioxidant and antibacterial effects

Corresponding author: Hakan Erdoğan, University of Health Sciences, Gülhane Faculty of Pharmacy, Department of Pharmaceutical Chemistry, Emrah Str., 06018, Etlik-Ankara/Turkey. ORCID: 0000-0002-7791-7445
E-mail: *hakan.erdogan@sbu.edu.tr*

of AgNPs formed on dipeptide structures. We also investigated the cytotoxic effects of Gly-His films in murine fibroblasts (L929).

MATERIALS AND METHODS

Chemicals

The chemicals used in the study were purchased from the following suppliers: Dulbecco's Modified Eagle Medium (DMEM) and Dulbecco's Phosphate-Buffered Saline (PBS) from Wisent (Saint-Jean-Baptiste, QC, Canada); trypsin-EDTA from Biological Industries (Beit-Haemek, Israel); foetal bovine serum (FBS) and penicillin-streptomycin from Capricorn Scientific (Ebsdorfergrund, Germany); and dimethyl sulphoxide (DMSO) and 2,2-diphenyl-1-picrylhydrazyl (DPPH) from Sigma-Aldrich Chemicals (Munich, Germany).

Preparation of Gly-His dipeptides in solvents

Gly-His dipeptides were dissolved in one of the following solvents: 1,1,1,3,3,3-hexafluoro-2-propanol (HFIP), ethanol, methanol, chloroform, tetrahydrofuran (THF), water, or acetone in the final concentration of 2 mg/mL and then dropped onto silicon discs. The solvent was evaporated at room temperature.

Preparation of AgNP-decorated Gly-His films

Gly-His dipeptides dropped onto the silicon disc were kept in 1 mmol/L $AgNO_3$ medium for 3, 6, 12, and 24 h to self-assemble. The discs were then removed from the silver medium, immersed in deionised water to remove residual ions, and then taken out to dry in room conditions.

Determination of antioxidant activity

Antioxidant activity of Gly-His dipeptides and AgNP-decorated Gly-His films was determined with the DPPH assay as described elsewhere (21). Briefly, DPPH solution was prepared by dissolving 6.0 mg of the compound in 100 mL of methanol. Then, various concentrations (0.5 mg/mL, 1 mg/mL, 2 mg/mL, 4 mg/mL, or 6 mg/mL) of 50 μL solutions of Gly-His dipeptide films with or without AgNPs were added to 150 μL of the prepared DPPH solution in 96-well plate. Ascorbic acid was used as standard and DPPH in methanol as blank. The plate was shaken and incubated in the dark for 30 min. After incubation, the absorbances of the solutions were measured with a microplate reader (BioTek Instruments, Winooski, VT, USA). Their scavenging activities were calculated as follows:

$$\text{Scavenging activity} = 100[(A_c - A_s)/A_c] \quad \text{[Equation 1]}$$

where A_c is the absorbance of control and A_s the absorbance of the standard or sample.

Cell culture

L929 cells (kindly provided by Ankara University Faculty of Pharmacy, Department of Pharmaceutical Toxicology, Ankara, Turkey) were seeded in 25 cm^2 flasks with 7 mL of DMEM supplemented with 10 % FBS and 1 % penicillin-streptomycin and then grown in an incubator (Sanyo, Japan) at 37 °C in an atmosphere supplemented with 5 % CO_2 for 24 h.

Cytotoxicity assay

Cytotoxicity was determined with the 3-(4,5-dimethylthiazol-2-yl)-2,5-diphenyltetrazolium bromide (MTT) assay as described earlier by Bacanli et al. (22). Following cell disaggregation with trypsin/EDTA and resuspension in medium, a total of 10^5 cells/well were plated in 96-well tissue-culture plates. The cells were incubated in full medium with various concentrations (0.5, 1, 2, 4, and 6 mg/mL) of AgNP-decorated Gly-His films at 37 °C in 5 % CO_2 in air for 24, 48, and 72 h. Full medium was used as negative control. After exposure, the medium was aspirated, cells washed with PBS, 10 μL of MTT (5 mg/mL of stock solution with PBS) added to 100 μL of cell suspension per well, and cells incubated for another 4 h. The MTT dye was then carefully removed, and 100 μL of DMSO added to each well. The absorbance of each well was measured with a microplate reader (BioTek Instruments) at 570 nm.

Preparation of AgNP-decorated Gly-His film-coated blank antibiotic discs

Gly-His dipeptide dropped onto Oxoid™ blank antimicrobial susceptibility discs, 6 mm in diameter (Thermo Scientific, Waltham, MA USA) in the final concentration of 2 mg/mL were kept in 1 mmol/L $AgNO_3$ medium for 3, 6, 12, and 24 h to self-assemble. The discs were then removed from the silver medium and immersed in deionised water to remove residual ions and then taken out to dry in room conditions.

Antibacterial activity

The activity of AgNP-decorated Gly-His dipeptide films against *Escherichia coli* ATCC 25922 (Gram-negative), *Staphylococcus aureus* ATCC 29213 (Gram-positive), and *Pseudomonas aeruginosa* ATCC 27853 (Gram-negative) was determined using the disc diffusion method recommended by the European Committee on Antimicrobial Susceptibility Testing (EUCAST) (23). Glycine-histidine dipeptide without AgNPs was used as negative control, and ciprofloxacin as positive control. Bacterial suspensions were prepared from fresh cultures to obtain 0.5 McFarland standard and 25 mL spread on each Mueller Hinton Agar (MHA) plate with a sterile swab. Prepared paper discs containing 2 mg/mL Gly-His with AgNPs accumulated for 3, 6, 12, or 24 h were placed on MHA plates and incubated at 35±1 °C for 18–20 h. The antibacterial activity of AgNPs was evaluated by measuring inhibition diameters and calculating the inhibition area (mm^2) around test discs.

Morphological and crystallographic characterisation

To characterise all dipeptide structures we coated the samples with a 5 nm Au-Pd layer and used a Quanta 400F Field-Emission Scanning Electron Microscope (FE-SEM, Thermo Fisher Scientific, Altrincham, UK) with an acceleration voltage of 20 kV and attenuated total reflection Fourier Transform Infrared (FTIR) spectrometer (Perkin Elmer, Waltham, MA, USA). Crystallographic features were also determined with the X-ray diffraction (XRD) (Ultima IV, Rigaku, Tokyo, Japan). Measurements were performed at Cu Kα radiation (40 kV and 30 mA). The scan rate was 2°/min and range 2.5-80°.

RESULTS AND DISCUSSION

Figure 1 shows SEM images of self-assembled Gly-His dipeptides dissolved in HFIP, water, ethanol, methanol, acetone, and THF. Most dipeptide moieties easily solved in all solvents. They generally assumed a film-like morphology, probably owing to hydrogen bonding between the N-H (NH_2 group) and O-H (COOH group) terminals of dipeptide molecules (24). However, their structures differ: dipeptides solved in HFIP self-assembled in a spherical structure (Figure 1a), and those dissolved in chloroform assumed square structure (Figure 1e). In addition, the film layer of dipeptides dissolved in acetone formed pores (Figure 1d). Continuous film layers were preserved in HFIP, water, and ethanol, which suggests that they have potential application as film biomaterials.

An earlier report suggests that polarity, hydrogen bonding capacity, and dielectric constants of solvents may be the driving forces in dipeptide self-assembly (6). In Gly-His dipeptides, the driving force are inter- and intra-molecular hydrogen bonds. The latter are possible due to the carboxylic acid and amine head groups, and they often take the form of a film. Weaker film formation is particularly common in solvents with low hydrogen-bonding capacity, such as chloroform and acetone. In this case, the effective driving force is thought to be the interaction between the hydroxyl groups of the amine and carboxylic acid (6).

Figure 2 shows similar FTIR spectra of the film-like Gly-His dipeptide structures, regardless of solvent. The primary amide band in the 1600–1700 cm^{-1} frequency range usually takes the α-helix, β-sheet, β-turn, or random-coil structure after self-assembly and is independent of the amino acid sequence, hydrophilic or hydrophobic properties of the system, or the skeletal structure and charge of the amino acid. In the β-sheet conformation, two prominent peaks arise around 1630 cm^{-1} and 1690 cm^{-1}. In the α-helix structure, primary amide band usually appears around 1650 cm^{-1} and in random-coil structure around 1648 cm^{-1}. The secondary amide band with the α-helix structure usually appears around 1545 cm^{-1} together with the primary band. Sharp peaks around 3250 cm^{-1} correspond to N-H stretching. In contrast, β-turned structure can be seen between 1660 and 1680 cm^{-1}. Broad peaks, especially around 3000–3500 cm^{-1},

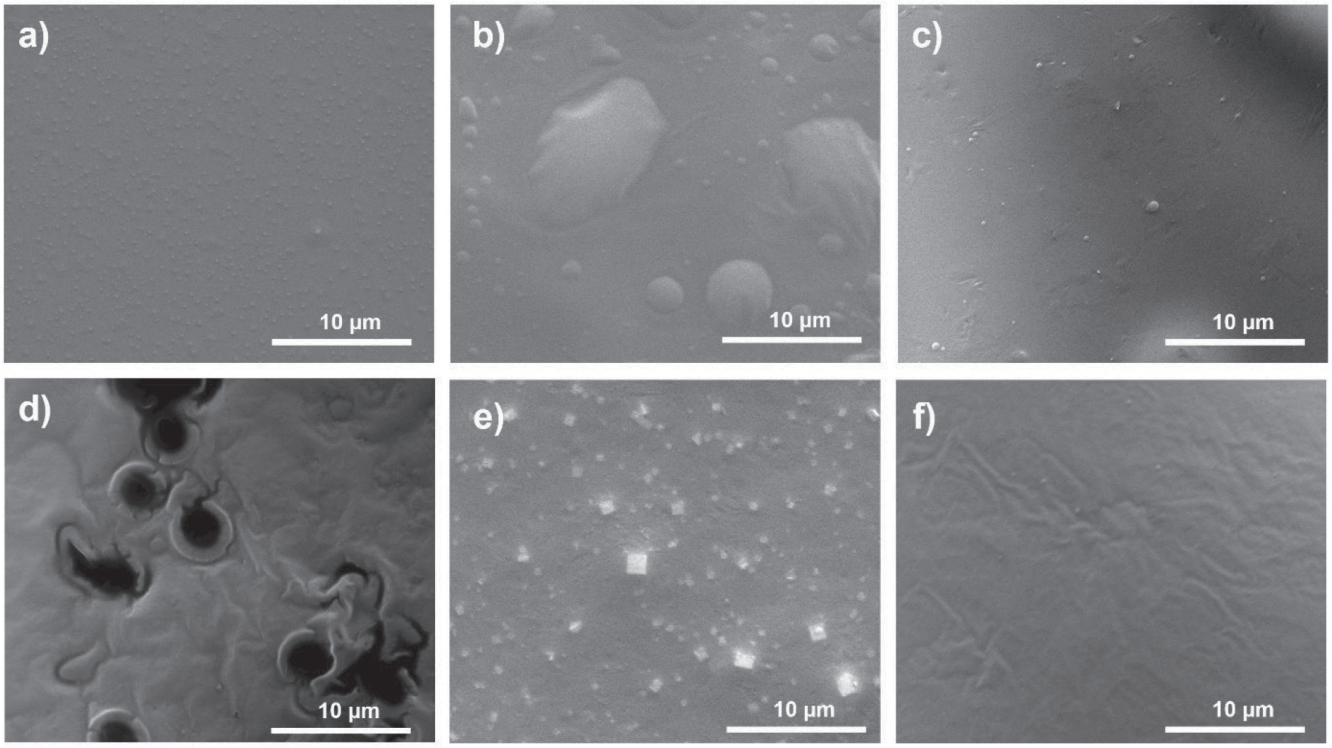

Figure 1 SEM image of self-assembled Gly-His dipeptide films in various solvents: a) 1,1,1,3,3,3-hexafluoro-2-propanol, b) water, c) ethanol, d) acetone, e) chloroform, and f) tetrahydrofuran

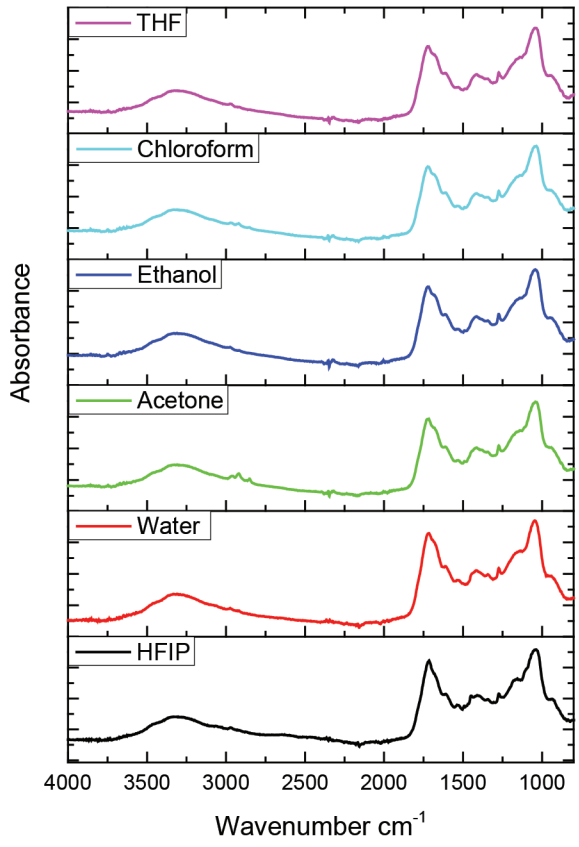

Figure 2 FTIR spectra of Gly-His dipeptide films self-assembled in various solvent media. HFIP – 1,1,1,3,3,3-hexafluoro-2-propanol; THF – tetrahydrofuran

are believed to originate from -OH and -NH groups (25, 26). The band around 1700 cm^{-1} is considered to be the C=O band. One of bands that explains the role of hydrogen bond interactions is the C=O band. The fact that these bands have remained similar in Figure 2 may indicate that self-assembly is owed to ionic and other weak interactions. Here, to examine the secondary morphology of these structures, the primary amide frequency range between 1600 and 1700 cm^{-1} should be examined, but this part cannot be seen in detail because the tight polymer-like film structure formed by the arrangement of Gly-His dipeptides gives a spectrum in the form of broad bands with behaviour specific to polymer structures.

Another feature of amino acid and dipeptide structures is that they can be decorated with different nano and microstructures by reducing or oxidising metal cations with a specific reduction potential. Several studies have investigated the capacity of Gly and His amino acids to form complexes with metal ions (27–31). Metal chelation, which often takes place, determines the antioxidant profile exhibited by several histidine-containing dipeptides (32). For this purpose, we prepared Gly-His dipeptide films in ethanol to examine their behaviour in the presence of the Ag ion and their antioxidant properties. Interestingly, their morphological properties changed, as can be seen in SEM images in Figure 3. The most notable is the rearrangement of fibres in the presence of $AgNO_3$ solution.

Figure 3b also shows the EDX spectra of Gly-His film kept in the $AgNO_3$ solution, in which the peaks point to C and O in the dipeptide structure. In addition, the rugged Si peak is caused by the Si wafer, which is the substrate of retaining.

Figure 4 shows time-related morphological changes of Gly-His dipeptide films left in the $AgNO_3$ medium for 0, 3, 6, 12, or 24 h. At 0 h, AgNPs take globular structure. At 3 and 6 h, AgNPs

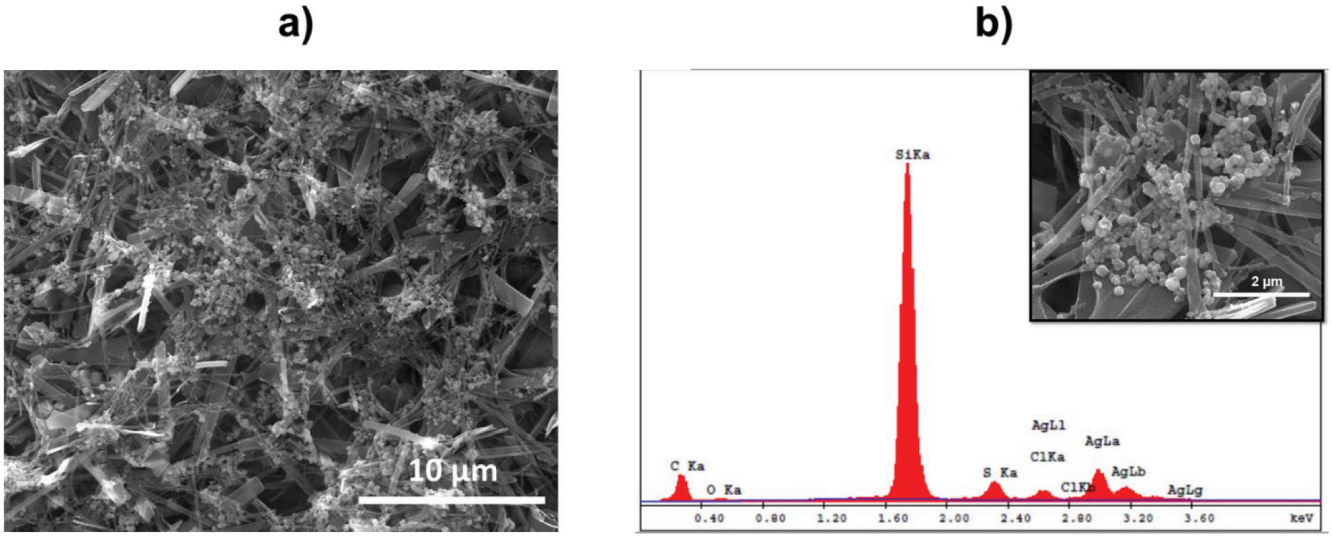

Figure 3 SEM images of (a) morphological changes in Gly-His films formed in $AgNO_3$ solutions for 6 h and (b) zoomed AgNP-decorated Gly-His structure with the EDX spectrum

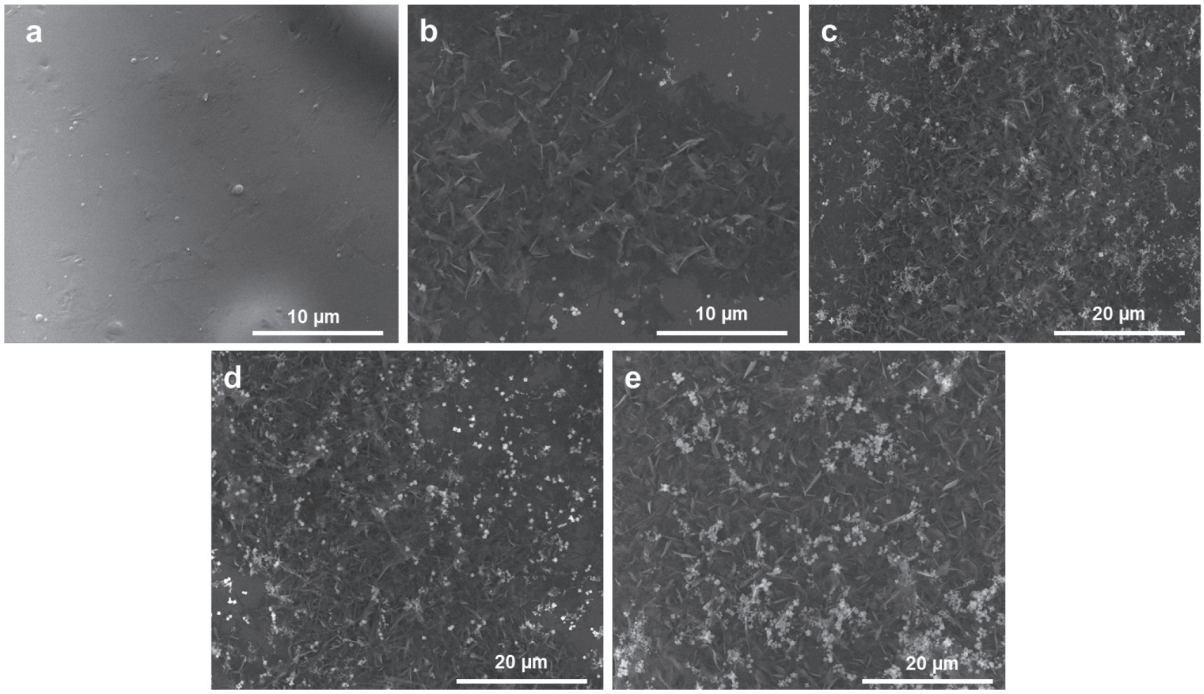

Figure 4 SEM images of Gly-His film structures kept in $AgNO_3$ solution for a) 0 h, b) 3 h, c) 6 h, d) 12 h, and e) 24 h

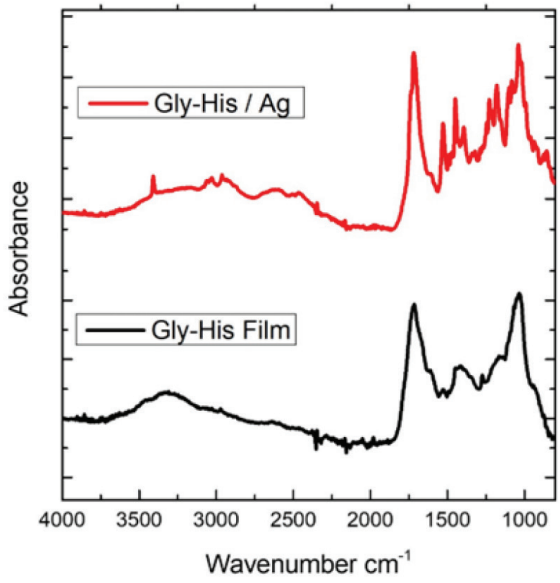

Figure 5 FTIR spectra of Gly-His dipeptide films with and without Ag

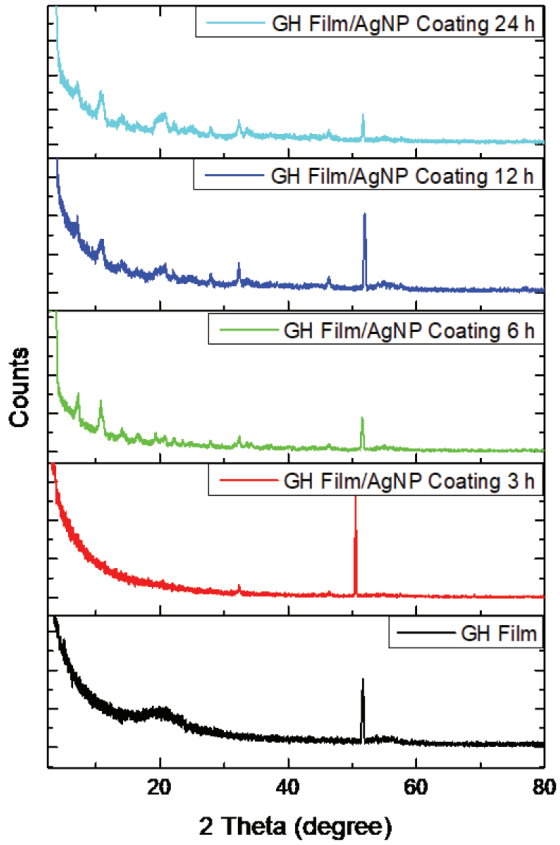

Figure 6 XRD spectra of Gly-His film alone or kept in $AgNO_3$ solution for various times

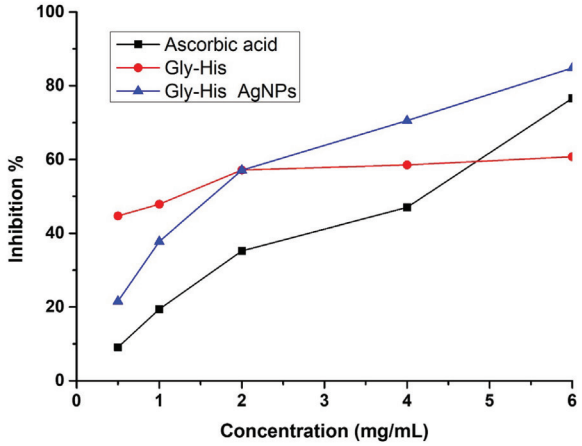

Figure 7 Antioxidant activity of Gly-His films alone and those coated with AgNPs

randomly scatter across the surface, still retaining their globular form. At 12 and 24 h, they deteriorate into needle-like and cube-like forms. These structures are formed at the end of the cooldown and may be collapsed AgNPs.

Figure 5 shows the FTIR spectra of AgNP-decorated Gly-His structures. The bands obtained around 1300–1500 cm^{-1} are more clearly separated. The peaks around 1700 cm^{-1} correspond to the COO- groups. The spectrum's peaks at 3000–3500 cm^{-1} correspond to the -OH and -NH groups.

Figure 6 shows the XRD patterns of AgNP-decorated Gly-His film at the four time points. At the angle range of 2θ (2.5−80°), Gly-His dipeptide film has an amorphous structure without distinct diffraction pattern, but in the presence of $AgNO_3$ it has transited to a needle and fibre-like structure. Sharp diffraction peaks are visible at 7.22, 10.65, 14.14, 16.40, 19.23, 27.86, 32.24, and 46.30 °. The d spacing values corresponding to these peaks are 12.24, 8.26, and 6.30, 5.39, 4.62, 3.20 2.77, and 1.96 Å, respectively. The same peaks at 27.86, 32.24, and 46.32 ° have already been reported for Ag_2O nanoparticles on a dipeptide surface by Babu et al. (33).

Similar to earlier studies (34–37), we found higher antioxidant activity of AgNP-decorated Gly-His films than ascorbic acid in the concentration range of 0–6 mg/mL (Figure 7).

There are various studies about the cytotoxic effects of AgNPs, but ours is the first to evaluate the cytotoxic effects of the Gly-His dipeptide, with and without AgNPs (Figure 8). The Gly-His dipeptide without AgNPs did not significantly lower L929 cell viability at hour 24, 48, and 72 of incubation, but the one with AgNPs did. The IC_{50} values of AgNP-decorated Gly-His films at 24, 48, and 72 h of exposure were 3.679 μg/mL, 3.251 μg/mL, and 3.096 μg/mL.

Antibacterial activity of AgNP-decorated Gyl-His dipeptide films turned out to be the most effective against *E. coli S. aureus*, and *P. aeruginosa* in dipeptide samples previously kept in the $AgNO_3$ solution for 24 h, and the effect was the most prominent against *P.*

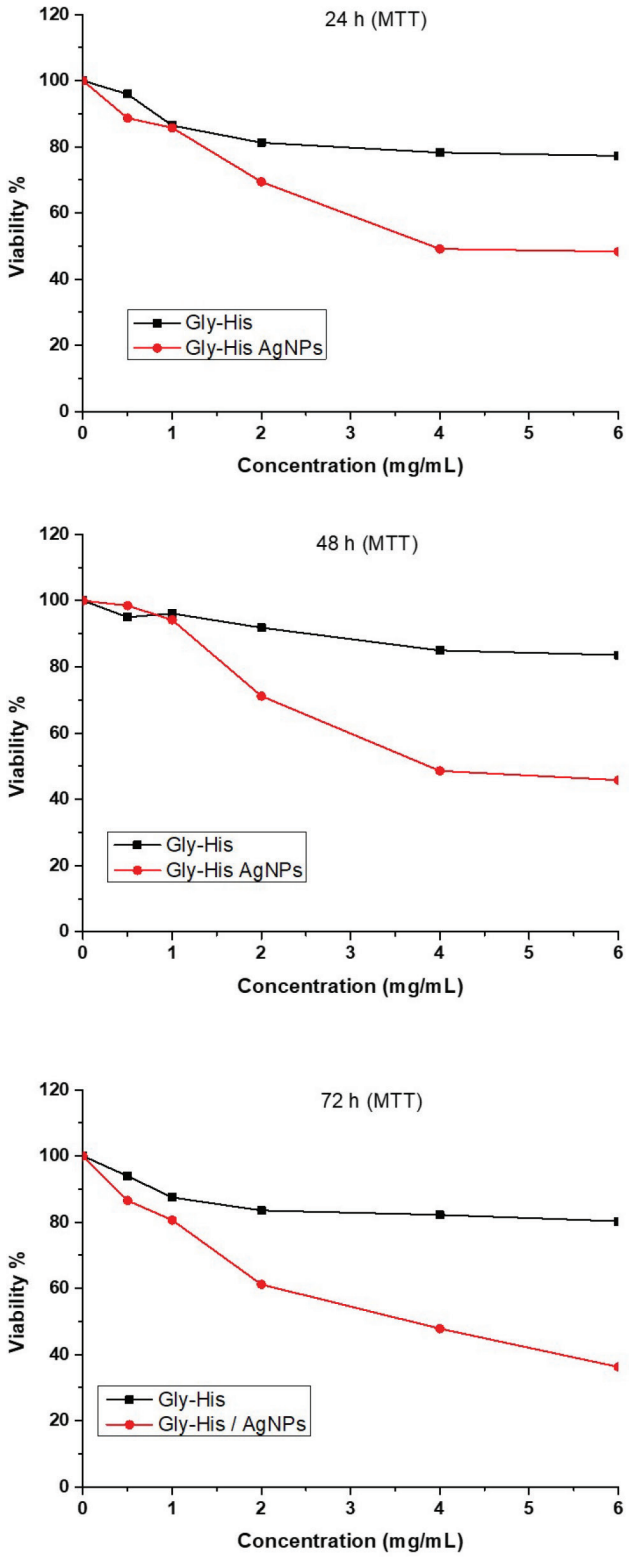

Figure 8 Cytotoxic effects of Gly-His dipeptide with and without AgNPs in L929 cells

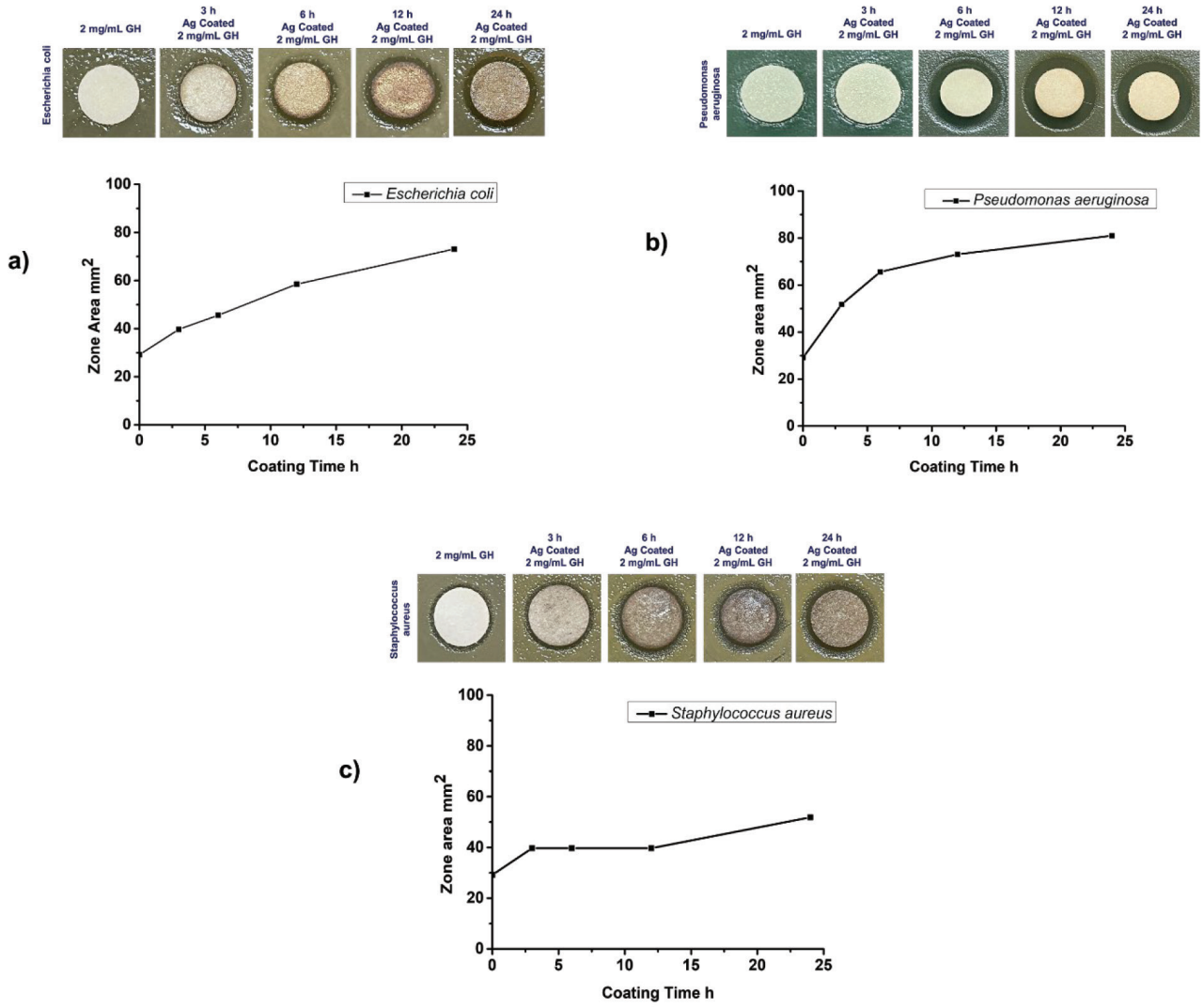

Figure 9 Antibacterial activity of Gly-His dipeptides with or without AgNPs against a) *Escherichia coli*, b) *Staphylococcus aureus*, and c) *Pseudomonas aeruginosa*

aeruginosa (Figure 9). These findings are in agreement with other studies involving AgNPs (19, 27, 38–42) and point to potential in future applications.

CONCLUSIONS

Our study has shown that the Gly-His dipeptides self-assemble as film-like structures through hydrogen-bond-induced rearrangement resulting in an amorphous flat layer. This film-like structure has potential, especially for topical applications, as it can coat wide surfaces. Pairing it with AgNPs can increase antibacterial activity of the film, without being toxic to other cells at concentrations below 2 mg/mL. However, further *in vivo* and clinical research is needed to prove that AgNP-decorated Gly-His films have antibacterial effects without toxic effects.

Conflict of interests

None to declare.

Acknowledgments

The authors are grateful to the Scientific Research Projects Unit of the University of Health Sciences Turkey for financial support under the Project No. 2020/10. We also wish to thank Professor Aylin Üstündağ from Ankara University Faculty of Pharmacy for helping us get the L929 cells.

REFERENCES

1. Wang L, Gong C, Yuan X, Wei G. Controlling the self-assembly of biomolecules into functional nanomaterials through internal interactions and external stimulations: a review. Nanomaterials (Basel) 2019;9(2):285. doi: 10.3390/nano9020285
2. Zou Q, Yan X. Amino acid coordinated self-assembly. Chemistry 2018;24:755–61. doi: 10.1002/chem.201704032
3. Hamley I. Self-assembly of amphiphilic peptides. Soft Matter 2011;7:4122–38. doi: 10.1039/C0SM01218A
4. Martin RB. Free energies and equilibria of peptide bond hydrolysis and formation. Biopolymers 1998;45:351–3. doi: 10.1002/(SICI)1097-0282(19980415)45:5<351::AID-BIP3>3.0.CO;2-K
5. Chan KH, Xue B, Robinson RC, Hauser CAE. Systematic moiety variations of ultrashort peptides produce profound effects on self-assembly, nanostructure formation, hydrogelation, and phase transition. Sci Rep 2017;7(1):12897. doi: 10.1038/s41598-017-12694-9
6. Erdogan H, Babur E, Yilmaz M, Candas E, Gordesel M, Dede Y, Oren EE, Demirel GB, Ozturk MK, Yavuz MS, Demirel G. Morphological versatility in the self-assembly of Val-Ala and Ala-Val dipeptides. Langmuir 2015;31:7337–45. doi: 10.1021/acs.langmuir.5b01406
7. Erdoğan H. Cation-based approach to morphological diversity of diphenylalanine dipeptide structures. Soft Matter 2021;17:5221–30. doi: 10.1039/D1SM00083G
8. Qin S-Y, Pei Y, Liy X-J, Zhuo R-X, Zhang X-Z. Hierarchical self-assembly of a β-amyloid peptide derivative. J Mater Chem B 2013;1:668–75. doi: 10.1039/C2TB00105E
9. Chen L, Morris K, Laybourn A, Elias D, Hicks MR, Rodger A, Serpell L, Adams DJ. Self-assembly mechanism for a naphthalene-dipeptide leading to hydrogelation. Langmuir 2010;26:5232–42. doi: 10.1021/la903694a
10. Erdogan H, Sakalak H, Yavuz MS, Demirel G. Laser-triggered degelation control of gold nanoparticle embedded peptide organogels. Langmuir 2013;29:6975–82. doi: 10.1021/la401300u
11. Sarmadi BH, Ismail A. Antioxidative peptides from food proteins: a review. Peptides 2010;31:1949–56. doi: 10.1016/j.peptides.2010.06.020
12. Zheng L, Zhao Y, Dong H, Su G, Zhao M. Structure-activity relationship of antioxidant dipeptides: Dominant role of Tyr, Trp, Cys and Met residues. J Funct Foods 2016;21:485–96. doi: 10.1016/j.jff.2015.12.003
13. Ambigaipalan P, Shahidi F. Antioxidant potential of date (*Phoenix dactylifera* L.) seed protein hydrolysates and carnosine in food and biological systems. J Agric Food Chem 2015;63:864–71. doi: 10.1021/jf505327b
14. Mukherjee M, Mahapatra A. Catalytic effect of silver nanoparticle on electron transfer reaction: Reduction of $[Co(NH_3)_5Cl](NO_3)_2$ by iron(II). Colloid Surface A 2009;350:1–7. doi: 10.1016/j.colsurfa.2009.08.021
15. Bajaj M, Pandey SK, Nain T, Brar SK, Singh P, Singh S, Wangoo N, Sharma RK. Stabilized cationic dipeptide capped gold/silver nanohybrids: Towards enhanced antibacterial and antifungal efficacy. Colloid Surface B 2017;158:397–407. doi: 10.1016/j.colsurfb.2017.07.009
16. Erdoğan H. Catalytic degradation of 4-Nitrophenol and methylene blue by bioinspired polydopamine coated dipeptide structures. Colloid Interface Sci Commun 2020;39:100331. doi: 10.1016/j.colcom.2020.100331
17. Aisida SO, Ugwu K, Nwanya AC, Bashir A, Nwankwo NU, Ahmed I, Ezema FI. Biosynthesis of silver oxide nanoparticles using leave extract of Telfairia occidentalis and its antibacterial activity. Mater Today Proc 2021;36:208–13. doi: 10.1016/j.matpr.2020.03.005
18. Hamouda T, Ibrahim HM, Kafafy HH, Mashaly HM, Mohamed NH, Aly NM. Preparation of cellulose-based wipes treated with antimicrobial and antiviral silver nanoparticles as novel effective high-performance coronavirus fighter. Int J Biol Macromol 2021;181:990–1002. doi: 10.1016/j.ijbiomac.2021.04.071
19. Mba IE, Nweze EI. Nanoparticles as therapeutic options for treating multidrug-resistant bacteria: research progress, challenges, and prospects. World J Microbiol Biotechnol 2021;37(6):108. doi: 10.1007/s11274-021-03070-x
20. Mohler JS, Sim W, Blaskovich MAT, Cooper MA, Ziora ZM. Silver bullets: A new lustre on an old antimicrobial agent. Biotechnol Adv 2018;36:1391–411. doi: 10.1016/j.biotechadv.2018.05.004
21. Tung Y-T, Wu J-H, Hsieh C-Y, Chen P-S, Chang S-T. Free radical-scavenging phytochemicals of hot water extracts of *Acacia confusa* leaves detected by an on-line screening method. Food Chem 2009;115:1019–24. doi: 10.1016/j.foodchem.2009.01.026
22. Bacanli M, Esim MO, Erdogan H, Sarper M, Erdem O, Ozkan Y. Evaluation of cytotoxic and genotoxic effects of paclitaxel-loaded PLGA nanoparticles in neuroblastoma cells. Food Chem Toxicol 2021;154:112323. doi: 10.1016/j.fct.2021.112323
23. European Committee on Animicrobial Susceptibility Testing EUCAST. Breakpoint tables for interpretation of MICs and zone diameters. Version 12.0, 2022 [displayed 9 June 2022]. Available at https://www.eucast.org/clinical_breakpoints/
24. To T, Sakamoto Y, Sadakane K, Matsugami M, Takamuku T. Aggregation of the dipeptide leu-gly in alcohol-water binary solvents elucidated from the solvation structure for each moiety. J Phys Chem B 2021;125:240–52. doi: 10.1021/acs.jpcb.0c08809
25. Ji W, Yuan C, Chakraborty P, Gilead S, Yan X, Gazit E. Stoichiometry-controlled secondary structure transition of amyloid-derived supramolecular dipeptide co-assemblies. Commun Chem 2019;2(1):65. doi: 10.1038/s42004-019-0170-z
26. Ji W, Yuan C, Zilberzwige-Tal S, Xing R, Chakraborty P, Tao K, Gilead S, Yan X, Gazit E. Metal-ion modulated structural transformation of amyloid-like dipeptide supramolecular self-assembly. ACS Nano 2019;13:7300–9. doi: 10.1021/acsnano.9b03444
27. Adebayo-Tayo B, Salaam A, Ajibade A. Green synthesis of silver nanoparticle using *Oscillatoria* sp. extract, its antibacterial, antibiofilm potential and cytotoxicity activity. Heliyon 2019;5(10):e02502. doi: 10.1016/j.heliyon.2019.e02502
28. Case DR, Zubieta J, Gonzalez R, Doyle RP. Synthesis and chemical and biological evaluation of a glycine tripeptide chelate of magnesium. Molecules 2021;26(9):2419. doi: 10.3390/molecules26092419
29. Elshafie HS, Sakr SH, Sadeek SA, Camele I. Biological investigations and spectroscopic studies of new moxifloxacin/glycine-metal complexes. Chem Biodivers 2019;16(3):e1800633. doi: 10.1002/cbdv.201800633
30. Maia MT, Sena DN, Calais GB, Luna FMT, Beppu MM, Vieira RS. Effects of histidine modification of chitosan microparticles on metal ion adsorption. React Funct Polym 2020;154:104694. doi: 10.1016/j.reactfunctpolym.2020.104694

31. Riguero V, Clifford R, Dawley M, Dickson M, Gastfriend B, Thompson C, Wang SC, O'Connor E. Immobilized metal affinity chromatography optimization for poly-histidine tagged proteins. J Chromatogr A 2020;1629:461505. doi: 10.1016/j.chroma.2020.461505
32. Hartman PE, Hartman Z, Ault KT. Scavenging of singlet molecular oxygen by imidazole compounds: high and sustained activities of carboxy terminal histidine dipeptides and exceptional activity of imidazole-4-acetic acid. Photochem Photobiol 1990;51:59–66. doi: 10.1111/j.1751-1097.1990.tb01684.x
33. Babu PJ, Doble M, Raichur AM. Silver oxide nanoparticles embedded silk fibroin spuns: Microwave mediated preparation, characterization and their synergistic wound healing and anti-bacterial activity. J Colloid Interface Sci 2018;513:62–71. doi: 10.1016/j.jcis.2017.11.001
34. Ahn EY, Jin H, Park Y. Assessing the antioxidant, cytotoxic, apoptotic and wound healing properties of silver nanoparticles green-synthesized by plant extracts. Mater Sci Engin C 2019;101:204–16. doi: 10.1016/j.msec.2019.03.095
35. Zhao X, Zhou L, Riaz Rajoka MS, Yan L, Jiang C, Shao D, Zhu J, Shi J, Huang Q, Yang H, Jin M. Fungal silver nanoparticles: synthesis, application and challenges. Crit Rev Biotechnol 2018;38:817–35. doi: 10.1080/07388551.2017.1414141
36. Demirbas A, Welt BA, Ocsoy I. Biosynthesis of red cabbage extract directed Ag NPs and their effect on the loss of antioxidant activity. Mater Lett 2016;179:20–3. doi: 10.1016/j.matlet.2016.05.056
37. Lewinski N, Colvin V, Drezek R. Cytotoxicity of nanoparticles. Small 2008;4:26–49. doi: 10.1002/smll.200700595
38. El Sayed MT, El-Sayed ASA. Biocidal activity of metal nanoparticles synthesized by *Fusarium solani* against multidrug-resistant bacteria and mycotoxigenic fungi. J Microbiol Biotechnol 2020;30:226–36. doi: 10.4014/jmb.1906.06070
39. Hamouda RA, Hussein MH, Abo-Elmagd RA, Bawazir SS. Synthesis and biological characterization of silver nanoparticles derived from the cyanobacterium *Oscillatoria limnetica*. Sci Rep 2019;9(1):13071. doi: 10.1038/s41598-019-49444-y
40. Hossain MM, Polash SA, Takikawa M, Shubhra RD, Saha T, Islam Z, Hossain S, Hasan MA, Takeoka S, Sarker SR. Investigation of the antibacterial activity and *in vivo* cytotoxicity of biogenic silver nanoparticles as potent therapeutics. Front Bioeng Biotechnol 2019;7:239. doi: 10.3389/fbioe.2019.00239
41. Hu X, Saravanakumar K, Jin T, Wang MH. Mycosynthesis, characterization, anticancer and antibacterial activity of silver nanoparticles from endophytic fungus *Talaromyces purpureogenus*. Int J Nanomedicine 2019;14:3427–38. doi: 10.2147/IJN.S200817
42. Huq MA. Green synthesis of silver nanoparticles using *Pseudoduganella eburnea* MAHUQ-39 and their antimicrobial mechanisms investigation against drug resistant human pathogens. Int J Mol Sci 2020;21(4):1510. doi: 10.3390/ijms21041510

Antioksidacijska, citotoksična i antibakterijska svojstva samosloživih glicinsko-histidinskih dipeptida sa srebrnim nanočesticama i bez njih u bioinspiriranom filmu

Posljednjih je godina mnogo pažnje posvećeno samosložívim strukturama temeljenim na dipeptidima, a posebno samoregulaciji tih struktura s različitim nizovima aminokiselina. U ovome smo ispitivanju htjeli ustanoviti djelovanje različitih otopina na slaganje struktura dipeptida glicin-histidin (GH). Prvo smo utvrdili morfološka svojstva tih GH filmova odležanih u različitim otapalima pomoću pretražne (skenirajuće) elektronske mikroskopije, a zatim i njihova strukturna svojstva pomoću infracrvene spektroskopije s Fourierovom transformacijom (FTIR). Zatim smo utvrdili djelovanje tih struktura u filmu na raspoređivanje srebrnih nanočestica (AgNP) te antioksidacijska i citotoksična svojstva filmova obogaćenih AgNP-ovima. Osim toga, ocijenili smo antibakterijsko djelovanje filmova, s Ag česticama i bez njih na Gram negativne bakterije *Escherichia coli* i *Pseudomonas aureginosa* te Gram-pozitivni *Staphylococcus aureus*. GH filmovi s Ag nanočesticama nisu bili značajno citotoksični pri koncentracijama nižima od 2 mg/mL, ali su iskazale antibakterijsko djelovanje. Stoga smatramo da se takvi dipeptidni filmovi sa srebrnim nanočesticama mogu sigurno primjenjivati protiv bakterija.

KLJUČNE RIJEČI: Ag; antibakterijska površina; *Escherichia coli*; *Pseudomonas aeruginosa*; *Staphylococcus aureus*; toksičnost